Electron transport and thermoelectric properties of layered perovskite $LaBaCo_2O_{5.5}$

2009 J. Phys.: Condens. Matter 21 056007

(http://iopscience.iop.org/0953-8984/21/5/056007)

J. Phys.: Condens. Matter **21** (2009) 056007 (5pp) doi:10.1088/0953-8984/21/5/056007

Electron transport and thermoelectric properties of layered perovskite $LaBaCo_2O_{5.5}$

Asish K Kundu[1,2,3], B Raveau[1], V Caignaert[1], E-L Rautama[1] and V Pralong[1]

[1] Laboratoire CRISMAT, ENSICAEN UMR6508, 6 Boulevard Maréchal Juin, F-14050 Caen Cedex 4, France
[2] Solid State Physics Laboratory, Defence Research and Development Organization, Lucknow Road, Timarpur, Delhi 110054, India

E-mail: asish.k@gmail.com

Received 13 November 2008
Published 12 January 2009
Online at stacks.iop.org/JPhysCM/21/056007

Abstract

We have investigated systematically the physical transport properties of layered 112-type cobaltite by means of electrical resistivity, magnetoresistance and thermopower measurements. In order to understand the complex transport mechanism of $LaBaCo_2O_{5.5}$, the data have been analysed using different theoretical models. The compound shows an electronic transition between two semiconducting states around 326 K, which coincides with the ferromagnetic transition. Interestingly, the system also depicts a significant magnetoresistance (MR) effect near the ferro/antiferromagnetic phase boundary and the highest value of MR is close to 5% at 245 K under ± 7 T. The temperature dependence of thermopower, $S(T)$, exhibits p-type conductivity in the 60 K $\leqslant T \leqslant$ 320 K range and reaches a maximum value of around 303 μV K^{-1} (at 120 K). In the low temperature antiferromagnetic region the unusual $S(T)$ behaviour, generally observed for the cobaltite series $LnBaCo_2O_{5.5}$ (Ln = rare earth), is explained by the electron magnon scattering mechanism.

(Some figures in this article are in colour only in the electronic version)

1. Introduction

The layered perovskite cobaltites of 112-type $LnBaCo_2O_{5.5}$ (Ln = rare earth) have been of great interest due to their rich physical properties and interesting structural phenomena associated with them [1–6]. In the layered cobaltites where the oxygen stoichiometry is '5.5', the average valence of the cobalt ion is Co^{3+}. This is particularly interesting because of the ordering of Co^{3+} ions in two different crystallographic sites corresponding to pyramidal and octahedral oxygen coordination [1, 3, 5, 6]. Importantly, the $LnBaCo_2O_{5.5}$ systems possess a layered crystal structure which consists of layers $[LnO_x]$–$[CoO_2]$–[BaO]–$[CoO_2]$ alternating along the c axis [1, 3, 5]. The ordering of Ln^{3+} and Ba^{2+} ions is favourable if the size difference is large between the cations; hence smaller size Ln^{3+} easily form a layered structure. In contrast, for La^{3+} ions the size difference with Ba^{2+} is smaller and, as a result, the disordered cubic perovskite [2] is more stable and it requires special conditions to synthesize the 112-type layered structure. Although the series has been investigated in detail for almost all lanthanide elements of the periodic table, interestingly there is no such report [1, 2] on the first member of this series, i.e. for the lanthanum phase ($LaBaCo_2O_{5.5}$). Very recently we have discovered $LaBaCo_2O_{5.5}$ in terms of neutron diffraction, electron microscopy and magnetic studies, which shows that the structure is 112-layered orthorhombic with G-type antiferromagnetic (AFM) ordering [6]. Therefore, in this paper we have investigated in detail the electron transport properties of $LaBaCo_2O_{5.5}$. Interestingly, the system exhibits an electronic transition between two semiconducting states at $T_{SC} \sim 326$ K, which coincides with a paramagnetic (PM) to ferromagnetic (FM) transition and below room temperature

[3] Author to whom any correspondence should be addressed.

there is another magnetic transition ($T_N \sim 260$ K) from the FM to AFM state [6]. We have also carried out magnetoresistance (MR), thermopower (Seebeck coefficient), $S(T)$, and thermal conductivity, $\kappa(T)$, measurements to investigate the electron transport properties of the system below T_{SC}. The latter are sensitive to the magnetic and electrical nature of charge carriers (hole/electron) and can give some valuable information which is absent in the magnetotransport measurements. Additionally, the $S(T)$ data is less affected due to the presence of grain boundaries, which often complicates the $\rho(T)$ data interpretation for polycrystalline samples. We noticed that, at room temperature, the system shows a relatively large positive value of the thermoelectric power (91 μV K^{-1}), while it has a low resistivity ($\sim$1.14 Ω cm at 300 K). Therefore, we have calculated the power factor [7], $S^2\sigma$, as well as the figure of merit (ZT) as characterized for thermoelectric materials by $ZT = S^2\sigma T/\kappa$, where S, $\sigma(\sim 1/\rho)$, κ and T represent thermopower, electrical conductivity, thermal conductivity and absolute temperature, respectively.

2. Experimental procedure

The polycrystalline sample was prepared by means of a soft-chemistry method and the characterizations were carried out as described in [6]. The magnetization, resistivity and thermopower measurements were carried out with a Quantum Design physical property measurement system (PPMS). The electrical measurements were carried out on a rectangular-shaped (7.10 $\times$ 2.85 $\times$ 2.14 mm^3) sample by a standard four-probe method and a home-made sample holder was used for thermoelectric power measurements (using a steady state technique).

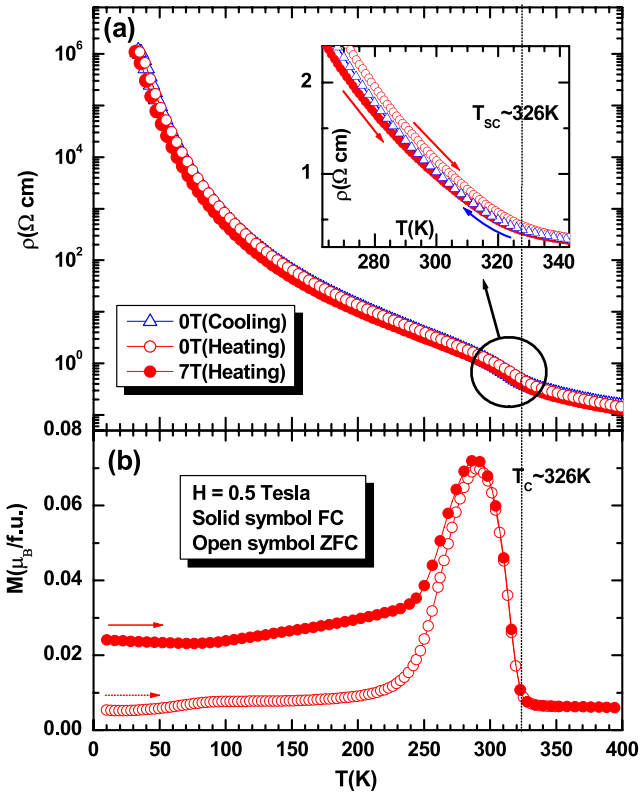

Figure 1. Temperature-dependent electrical and magnetic properties of ordered $LaBaCo_2O_{5.5}$: (a) electrical resistivity, $\rho(T)$, in the presence (solid symbol) and absence (open symbol) of magnetic field (7 T) during heating (circle) and cooling (triangle) cycles (inset shows the expanded version near the transition temperature, T_{SC}) and (b) ZFC (open symbol) and FC (solid symbol) magnetization, $M(T)$, in an applied field of 0.5 T.

3. Results and discussion

Figure 1 shows the temperature dependence of electrical resistivity, $\rho(T)$, and magnetization, $M(T)$, for $LaBaCo_2O_{5.5}$ in the temperature range of 10–400 K. The $\rho(T)$ data is collected during the heating and cooling cycle of the measurements in the presence and absence of an external magnetic field of 7 T. The zero-field $\rho(T)$ curve shows a significant change in slope corresponding to the semiconductor–semiconductor transition (T_{SC}) around 326 K (figure 1(a)). This type of transition was previously reported for the other series of $LnBaCo_2O_{5.5}$ [1–5] and referred to as the insulator–metal transition (T_{IM}), albeit the true nature of this transition is semiconducting to semiconducting type. For the present $LaBaCo_2O_{5.5}$ system, in contrast to a metallic behaviour, the slope of the resistivity curve ($d\rho/dT$) is negative above the transition temperature ($T > T_{SC}$), analogous to the $YBaCo_2O_{5.45}$ system [4]. Furthermore, for $LaBaCo_2O_{5.5}$ in an applied field of 7 T we did not observe any significant change in the resistivity behaviour throughout the temperature range, apart from a slight reduction in the magnitude below T_{SC}. It is observed (from figure 1) that the electronic and magnetic transition temperatures for $LaBaCo_2O_{5.5}$ are almost the same (T_C and $T_{SC} \approx 326$ K), quite the opposite to other perovskite cobaltites $LnBaCo_2O_{5.5}$, which exhibit a large shift between T_C and T_{IM} [1, 2]. We have re-investigated the magnetic properties of $LaBaCo_2O_{5.5}$: the zero-field-cooled (ZFC) and field-cooled (FC) magnetization data ($H = 0.5$ T) are shown in figure 1(b), which depicts two characteristic magnetic transitions. The common feature of the present study is the significant thermomagnetic irreversibility below the FM transition T_C and the presence of a weak magnetic transition at low temperature, which may be due to the coexistence of FM and AFM phases as reported earlier [6]. Hence, the sample is a magnetic semiconductor below T_{SC} and the resistivity increases exponentially with decreasing temperature. The high temperature ($T > T_{SC}$) resistivity behaviour is faintly temperature-dependent and is not affected by the magnetic field or measurement cycling process. As can be seen from the inset in figure 1(a), the $\rho(T)$ curves for cooling (triangle symbol) and heating (circle symbol) cycles illustrate only a small divergence below T_{SC} and merge above this temperature.

The semiconductor-or insulator-like transport in perovskite cobaltites can be characterized by three possible models [5, 8], namely thermal activation (TA): $\log\rho \propto 1/T$, Efros–Shklovskii-type hopping (ESH): $\log\rho \propto T^{-1/2}$ and Mott's variable range hopping (VRH): $\log\rho \propto T^{-1/4}$. To understand the transport mechanism for $LaBaCo_2O_{5.5}$, the data has been analysed based on these models. The zero-field resistivity data is plotted in figure 2, which shows that

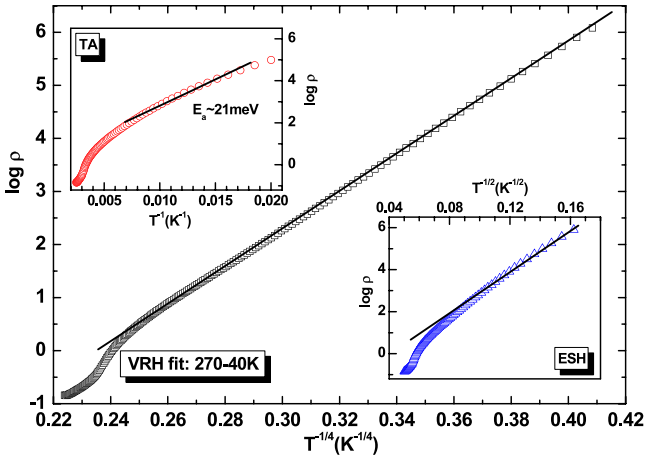

Figure 2. Logarithm of the resistivity versus $T^{-1/n}$ plots (where $n = 1$, 2 or 4) for ordered $LaBaCo_2O_{5.5}$: open symbols and solid lines represent the experimental data and apparent fit to the different hopping models as described in the text.

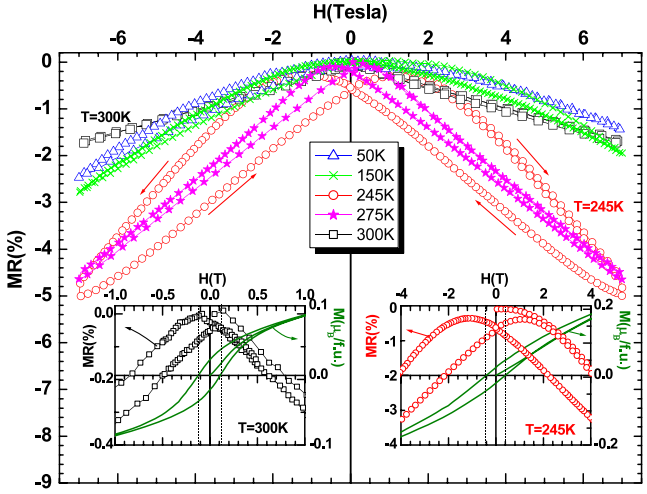

Figure 3. Magnetic-field-dependent isotherm magnetoresistance, MR, effect for ordered $LaBaCo_2O_{5.5}$ at five different temperatures ($H = \pm 7$ T). The inset figures show the isotherm magnetization, $M(H)$, and MR plot at 245 and 300 K for comparison; the dotted vertical lines represent the coercive field values.

the VRH model fits better than the other two models in the 40 K $\leqslant T \leqslant$ 270 K range, and is consistent with the preceding studies on perovskite cobaltites [5, 8]. This type of transport mechanism is typical for disordered systems, where the charge carriers move by hopping between localized states [8]. Taskin *et al* [5] have described the formation of localized states in terms of oxygen defects in $GdBaCo_2O_{5.5}$, which inevitably generate electrons or holes in the CoO_2 planes. Furthermore, we apply ESH and TA models, which are expected to describe the dominant conduction process. The transport mechanism is very complicated in the whole temperature region and does not satisfy entirely any of the above models. It can be seen from the inset of figure 2 that near or above room temperature they diverge from experimental data points. From the nearly linear region of the TA model ($T \leqslant 250$ K) we have calculated the approximate activation energy (E_a) of around 21 meV, yet less than the value reported for $GdBaCo_2O_{5.5}$ [5].

Figure 3, shows the magnetic-field-dependent isothermal magnetoresistance (MR) effect for $LaBaCo_2O_{5.5}$ at five different temperatures. Unfortunately, in the case of temperature-dependent resistivity data (with field), we did not observe any major change in the $\rho(T)$ curve even though the $M(T)$ behaviour reveals some kind of FM and AFM ordering [6]. The charge transport for this kind of system is expected to be very sensitive due to the coexistence of FM and AFM states and the external magnetic fields readily induce an MR effect by affecting the subtle balance between FM and AFM phases. Therefore, we have studied the isothermal MR effect at different temperatures and an apparent magnetic-field-dependent change in the MR is noticed below T_{SC}. The MR value is calculated [9] as $\mathrm{MR}(\%) = [\{\rho(7) - \rho(0)\}/\rho(0)] \times 100$, where $\rho(0)$ is the sample resistivity at 0 T and $\rho(7)$ in an applied field of 7 T. The highest negative MR value is obtained around -5% at 245 K in an applied field of 7 T and near room temperature the value is only -1.6%. At low temperatures, the MR values are only -2.8% (at 150 K) and -2.5% (at 50 K), respectively. The evidence of negative MR at low temperatures, similar to the tunnelling MR observed usually in polycrystalline samples for hole-doped cobaltites, is considered to be related to the spin-dependent scattering at grain boundaries. Nevertheless, in the present case the highest MR value is noticed near the FM–AFM phase boundary and hence the grain boundary effect can be ignored and considered to be an intrinsic effect. Interestingly, the magnetic-field-dependent isothermal MR behaviour at 245 K exhibits an irreversible effect analogous to those of isothermal magnetization, $M(H)$, behaviour (see inset figure 3), which is also present in 300 K isothermal MR data. The peak in the isothermal MR data occurs around the coercive field value, which corresponds to the state of maximum disorder in the orientation of the neighbouring magnetic spins. Hence, the field-dependent MR data that is indirectly related to the alignment between magnetic spins reaches a maximum value. This effect is prominent for 300 K data, compared to 245 K as shown from the inset in figure 3 (dotted vertical lines), which may be due to an FM-like state near 300 K whereas the latter one corresponds to a magnetic phase boundary. Additionally, the isothermal MR data exhibits hysteresis effects that resemble the 'butterfly-like' feature, although the effect is rather weak at low temperature (50 K). It is clear from the obtained data that the MR effect is strongly irreversible near the FM–AFM phase boundary (studied at 245 and 275 K). The 'butterfly-like' feature appears only near the magnetic phase boundary. Hence, the occurrences of irreversible MR behaviour nearly at similar temperatures to those for magnetic field variation isothermal $M(H)$ studies suggest the strongly correlated nature of field-induced magnetic and electronic transitions, as reported earlier for nanoscale ordered $LaBaCo_2O_6$ [9].

In order to get more insight into the nature of the conduction mechanism below T_{SC}, we have carried out thermoelectric power measurements. This is a simple and sensitive technique to investigate the scattering mechanism in electronic conduction, as discussed earlier. The temperature

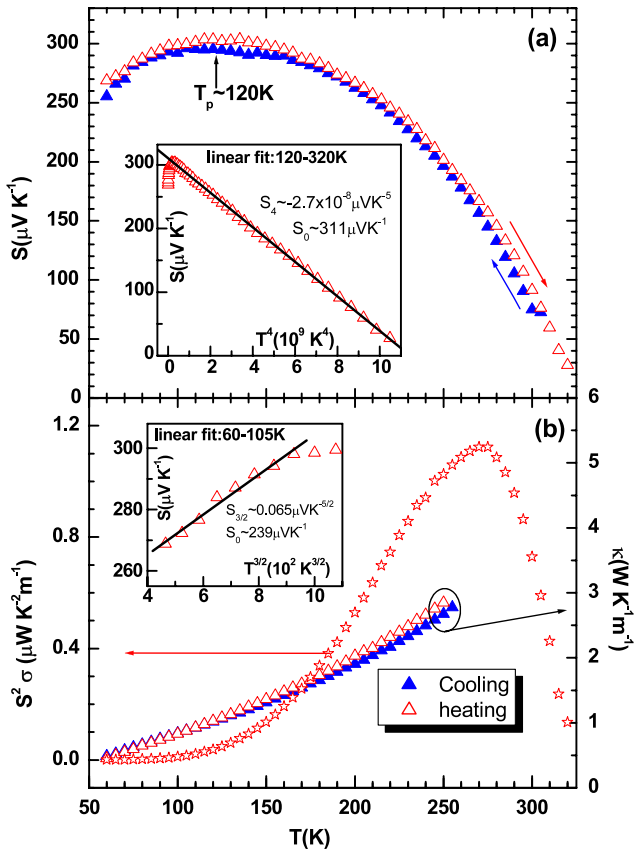

Figure 4. Temperature-dependent measurements for ordered $LaBaCo_2O_{5.5}$: (a) thermoelectric power, $S(T)$, during cooling (solid triangle) and heating (open triangle) cycles and inset shows the S–T^4 plot as discussed in the text, and (b) thermal conductivity, $\kappa(T)$, and power factor, $S^2\sigma(T)$, plots (inset shows the S–$T^{3/2}$ plot).

dependence of thermopower, $S(T)$, for cooling and heating cycles is shown in figure 4(a). It is observed that the $S(T)$ value is positive below T_{SC} and with decreasing temperature the value increases gradually and reaches a maximum value of $\sim$303 μV K^{-1} at around 120 K (referred to as T_P; marked by an arrow in the figure). Below T_P, the $S(T)$ value decreases continuously and due to the limitation of our instrument we could not obtain data below 60 K. We have also investigated the $S(T)$ evolution for another layered cobaltite $EuBaCo_2O_{5.5}$ (data not shown), which depicts similar features with $T_P \sim 90$ K. Consequently, from the literature values (i.e. for $NdBaCo_2O_{5.5}$, $GdBaCo_2O_{5.5}$ and $HoBaCo_2O_{5.5}$ the approximate T_P values are 105, 88 and 70 K, respectively [3, 5]) along with our present data we have plotted T_P as a function of different rare earth sizes. We obtain a linear decrease of T_P on decreasing the rare earth size (data not shown), which may be related to the decrease in bandwidth or increasing the energy bandgap with rare earth size. It is well known that the average cation size plays a crucial role in electronic conduction due to the change in electronic bandwidth as reported in the literature for disorder cobaltites [8].

The $S(T)$ data implies that the $LnBaCo_2O_{5.5}$ systems show a semiconducting type behaviour of the thermopower down to T_P akin to resistivity behaviour (figure 1(a)) and below T_P the $S(T)$ behaviour is complex, decreasing abruptly at low temperature. In fact, with decreasing temperature the $S(T)$ value should increase due to trapping or localization of charge carriers. This type of $S(T)$ behaviour is quite unexpected for semiconducting thermoelectric materials and there is no general explanation to date. Following the general approach in analysing the semiconducting behaviour we have plotted the $S(T)$ data in the $T^{-1/n}$ scale similar to $\rho(T)$. Since for semiconductors the $S(T)$ is expected to be linear in T^{-1} behaviour (according to the TA model) or to follow either of the described hopping models similar to resistivity behaviour [5, 8]. The plots show that the fitting (not shown) is very poor even for a short temperature range. Therefore, the $S(T)$ data cannot be described by the previous mentioned models and one observes p-type conductivity throughout the temperature range. Many authors have already explained the $S(T)$ behaviour at higher temperature and their sign reversal near the electronic transition [3, 5]. However, the low temperature $S(T)$ evolution, basically the appearance of the broad maximum (T_P) in the metastable AFM phase and the decreasing nature with temperature (in spite of the semiconducting behaviour), has not been explained properly. In this respect it is important to investigate the present system below room temperature. We have analysed the obtained thermopower data using an expression $S(T) = S_0 + S_{3/2}T^{3/2} + S_4T^4$ defined by Mandal [10], which can be understood on the basis of electron magnon scattering (spin wave theory). In ferro- and antiferromagnets, electrons are scattered by spin waves as explained earlier for perovskite manganites [10] and hence it is expected that this theory may explain the $S(T)$ behaviour for the present system. However, the obtained thermopower value is higher than that reported for manganites. The $S(T)$ curve shows a positive curvature below T_P and in the 60 K $\leqslant T \leqslant$ 105 K range the $S(T)$ data follows $T^{3/2}$ behaviour and in the 120–320 K range it fits linearly with the T^4 behaviour (insets of figure 4). The corresponding fitting coefficients $S_{3/2}$ and S_4 are 65×10^{-3} μV K$^{-5/2}$ and -2.7×10^{-8} μV K^{-5}, respectively, and the obtained values are one order of magnitude higher than the manganites [10]. At low temperature the second term ($S_{3/2}$) will dominate over S_4 ($S_{3/2} \gg S_4$) and hence the $S(T)$ will depict a downward trend below T_P. Although we do not have sufficient experimental data points below the broad peak, the $S(T)$ curve below T_P still fits linearly to the $T^{3/2}$ term (inset of figure 4(b)), as expected from the spin wave theory. Additionally, the downward feature in $S(T)$ data is present in all studied $LnBaCo_2O_{5.5}$ cobaltites [3, 5]. Hence, the broad peak at low temperature and downward trends for layered cobaltites are considered to be the result of the electron magnon scattering akin to perovskite manganite as explained by Mandal [10].

The temperature-dependent thermal conductivity, $\kappa(T)$, measurements of $LaBaCo_2O_{5.5}$ during cooling and heating cycles is shown in figure 4(b). We have plotted the data up to 250 K, as beyond this temperature the $\kappa(T)$ measurements are affected by thermal radiation effects. The $\kappa(T)$ value increases with increasing temperature, indicating an usual phonon-mediated scattering mechanism of charge carriers, which is the sum of phonon (κ_p) and electronic (κ_e) contributions

(i.e. $\kappa(T) = \kappa_p(T) + \kappa_e(T)$). Therefore, from the Wiedemann–Franz law we have calculated the electronic contribution (κ_e) at 250 K, which is around $\sim 1.5 \times 10^{-4}$ W K^{-1} m^{-1} (whereas κ (250 K) $\sim$ 2.8 W K^{-1} m^{-1}). This implies that the lattice-modulated phonon contribution (κ_p) is dominant near room temperature, i.e. $\kappa_p(T) \gg \kappa_e(T)$. We have also calculated the temperature dependence of power factor ($S^2\sigma$) from the obtained resistivity and thermopower data as shown in figure 4(b), which depicts a clear maximum near 270 K and decreases rapidly on both sides of the temperature scale (60 K $\leqslant T \leqslant$ 320 K). It is important to note that this maximum is in the region of the FM–AFM phase boundary. This suggests that the electron magnon scattering at low temperature strongly affects the $S(T)$ behaviour of the $LaBaCo_2O_{5.5}$ system. The calculated figure of merit (ZT) shows too small values close to room temperature ($\sim 10^{-5}$) for applications, as expected from 112-type cobaltite systems.

4. Conclusions

The prime result of current investigations is the unusual $S(T)$ behaviour at low temperature and the appearance of a broad peak around 120 K with a positive value of $\sim$303 μV K^{-1}. This is explained by the electron magnon scattering mechanism, which is expected to be applicable to all series of $LnBaCo_2O_{5.5}$ cobaltites at low temperature. Moreover, the magnetic-field-dependent isothermal MR data exhibits an irreversible feature with the highest value of MR around 5% (at 245 K and 7 T) near the FM–AFM phase boundary. The peak in the MR data appears close to the coercive field value, suggesting maximum domain wall interactions. This implies a strongly correlated nature of the magnetic and electron transport properties.

Acknowledgments

AKK gratefully acknowledges Drs A Pautrat and S Hebert for valuable suggestions during measurements and also for carefully reading this manuscript. The authors thank the CNRS and the French Ministry of Education and Research for financial support.

References

[1] Maignan A, Martin C, Pelloquin D, Nguyen N and Raveau B 1999 *J. Solid State Chem.* **142** 247
Seikh M M, Simon C, Caignaert V, Pralong V, Lepetit M B, Boudin S and Raveau B 2008 *Chem. Mater.* **20** 231
[2] Roy S, Dubenko I S, Khan M, Condon E M, Craig J, Ali N, Liu W and Mitchell B S 2005 *Phys. Rev.* B **71** 024419
[3] Maignan A, Caignaert V, Raveau B, Khomskii D and Sawatzky G 2004 *Phys. Rev. Lett.* **93** 26401
[4] Akashoshi D and Ueda Y 2001 *J. Solid State Chem.* **156** 355
Pautrat A, Boullay P, Hebert S and Caignaert V 2007 *Phys. Rev.* B **76** 214416
[5] Taskin A A, Lavrov A N and Ando Y 2005 *Phys. Rev.* B **71** 134414
Taskin A A, Lavrov A N and Ando Y 2006 *Phys. Rev.* B **73** 121101(R)
[6] Rautama E-L, Caignaert V, Boullay P, Kundu A K, Pralong V, Karppinen M, Ritter C and Raveau B 2009 *Chem. Mater.* **21** 102–9
[7] Terasaki I, Sasago Y and Uchinokura K 1997 *Phys. Rev.* B **56** 12685(R)
[8] Kundu A K, Ramesha K, Seshadri R and Rao C N R 2004 *J. Phys.: Condens. Matter* **16** 7955 and references therein
[9] Kundu A K, Rautama E-L, Boullay P, Caignaert V, Pralong V and Raveau B 2007 *Phys. Rev.* B **76** 184432
[10] Mandal P 2000 *Phys. Rev.* B **61** 14675